Talanta 116 (2013) 611–618

Contents lists available at ScienceDirect

Talanta

journal homepage: www.elsevier.com/locate/talanta

Homogenous detection of fumonisin B_1 with a molecular beacon based on fluorescence resonance energy transfer between $NaYF_4$: Yb, Ho upconversion nanoparticles and gold nanoparticles

Shijia Wu [a], Nuo Duan [a], Xiangli Li [b], Guiliang Tan [c], Xiaoyuan Ma [a], Yu Xia [a], Zhouping Wang [a,*], Hongxin Wang [a,*]

[a] State Key Laboratory of Food Science and Technology, School of Food Science and Technology, Jiangnan University, Wuxi 214122, China
[b] Department of Biomedicine, Zhongshan Torch Technology College, Zhongshan 528436, China
[c] Zhongshan Supervision Testing Institute of Quality & Metrology, Zhongshan 528403, China

ARTICLE INFO

Article history:
Received 1 March 2013
Received in revised form
28 June 2013
Accepted 9 July 2013
Available online 27 July 2013

Keywords:
Fumonisin B_1
$NaYF_4$: Yb
Ho upconversion nanoparticles
Gold nanoparticles
Fluorescence resonance energy transfer
Molecular beacons

ABSTRACT

In this work, we presented a new aptasensor for fumonisin B_1 (FB_1) based on fluorescence resonance energy transfer (FRET) between $NaYF_4$: Yb, Ho upconversion fluorescent nanoparticles (UCNPs) and gold nanoparticles (AuNPs). The quenchers (AuNPs) were attached to the 5′ end of the molecular beacon (MB), and the donors (UCNPs) were attached to the 3′ end of the MB. In the absence of target DNA (DNA complementary to FB_1 aptamers), the energy donors and acceptors were placed in close proximity, leading to quenching of the fluorescence of the UCNPs. Due to the combination of FB_1 and FB_1-specific aptamers, this caused some complementary DNA dissociating from the magnetic nanoparticles (MNPs). In the presence of the complementary DNA, the MBs underwent spontaneous conformational change and caused the UCNPs and AuNPs to detach from each other, resulting in restoration of the upconversion fluorescence. Therefore, the fluorescence of UCNPs was restored in a FB_1 concentration-dependent manner, which was the basis of the FB_1 quantification. The aptasensors showed a linear relationship from 0.01 to 100 ng mL^{-1} for FB_1 with a detection limit of 0.01 ng mL^{-1} in an aqueous buffer. As a practical application, the aptasensor was used to monitor FB_1 levels in naturally contaminated maize samples. The results were consistent with that of a classic ELISA method, indicating that the UCNPs–FRET aptasensor, which benefited from the near infrared excitation of $NaYF_4$: Yb, Ho UCNPs, was effective for directly sensing FB_1 in foodstuff samples without optical interference. This work also created the opportunity to develop aptasensors for other targets using this FRET system.

1. Introduction

Fluorescence quenching-based turn-on assay is one of the most important applications among various fluorescence resonance energy transfer (FRET)-based techniques, in which the fluorescence of the donor can be effectively quenched by the acceptor in the absence of targets. The quenched fluorescence will be "turned-on" upon addition of targets, and the restored fluorescence intensity will be proportional to the concentration of the targets. In recent years, FRET-based analytical methods have gained considerable attention as powerful tools for biological detection, including the widely used molecular beacon (MB) and TaqMan probes [1,2], because of their simplicity and high sensitivity. The MB has a hairpin-like stem–loop structure that contains both the fluorophore and quencher moieties [3,4]. In the absence of target DNA, the fluorophore and the quencher are in close proximity and the fluorescence from the MBs is quenched. In the presence of target DNA, the MB opens to form a double stranded DNA structure that separates the fluorophore and the quencher, leading to the restoration of fluorescence.

There are a number of conventional fluorescent biolabels used in FRET-based biological detection including organic dyes and fluorescent proteins [5]. However, such FRET-based assays generally suffer from photobleaching of traditional dyes, high autofluorescence background originating from the bio-species to be determined, and the inner filter effects caused by the absorbing species, all of which will greatly limit the detection sensitivity [6,7]. At present, most researchers focus their attention on finding the perfect donor–acceptor pair to improve FRET efficiency.

Lanthanide-doped, near-infrared-to-visible upconversion nanoparticles (UCNPs) are capable of emitting strong visible fluorescence

* Corresponding authors. Tel./fax: +86 510 85917023.
E-mail addresses: wangzp@jiangnan.edu.cn, wangzp1974@hotmail.com (Z. Wang).

0039-9140/$ - see front matter © 2013 Elsevier B.V. All rights reserved.
http://dx.doi.org/10.1016/j.talanta.2013.07.016

under the excitation of NIR light (typically 980 nm). They have significant advantages over traditional organic fluorophores as fluorescent biolabels due to their attractive optical and chemical features, including low toxicity, large stokes shifts, high resistance to photobleaching, blinking, and photochemical stability. In addition, they do not induce auto-fluorescence or a light scattering background [8,9]. As a result, the signal-to-background ratio and sensitivity of detection can be greatly improved. These advantages have made UCNPs an ideal choice recently as the fluorescence donor in the FRET-based turn-on assay [10–13].

Fumonisins are a group of mycotoxins primarily produced by Fusarium fungi, in particular Fusarium moniliforme and Fusarium proliferatum, which are some of the most common fungi in the world that form colonies on corn [14,15]. FB_1 is a nephrotoxin in all species tested, as well as a carcinogen and reproductive toxicant in rodents, and is thus likely to have the same effects in humans. Given its toxicity and prevalence, several analytical methods have been reported for the detection of FB_1. These include chromatographic methods such as TLC, LC and LC–MS, GC–MS, and HPLC [16,17]; enzyme-linked immunosorbent assays [18]; and capillary zone electrophoresis [19]. While these methods are effective, they require highly trained personnel and expensive equipment and are time-consuming, thus making them inaccessible for all but the most well-equipped laboratories and impractical for rapid testing on the spot [20].

In this study, we report a novel and simple FRET technique based on dual-functionalised molecular beacon. Although this work was not the first example of using a UCNPs-based FRET system for detection [11,13,21,22]. Now, we have designed advanced methods to detect fumonisin B_1 using $NaYF_4$: Yb, Ho upconversion nanoparticles as the donor, gold nanoparticles as the quencher and tight-binding aptamers for FB_1, which could be an important tool for sensing. And we also promoted the application of the aptamers.

2. Materials and methods

2.1. Reagents and apparatus

Rare-earth oxides used in this work, including yttrium oxide (Y_2O_3), ytterbium oxide (Yb_2O_3) and holmium oxide (Ho_2O_3) were of 99.99% purity. Hydrofluoric acid (HF), ferric trichloride ($FeCl_3 \cdot 6H_2O$), trisodium citrate ($Na_3C_6H_5O_7$), hydrogen tetrachloroaurate (III) ($HAuCl_4$), 25% ammonia ($NH_3 \cdot H_2O$), sodium hydroxide (NaOH), nitric acid (HNO_3), cetyltrimethyl ammonium bromide (CTAB), ethylene diamine tetraacetic acid (EDTA), 25% glutaraldehyde (OHC $(CH_2)_3$CHO) and tetraethyl orthosilicate (TEOS) were of analytical grade. All of the above chemicals were purchased from Sinopharm Chemical Reagent Co., Ltd. (Shanghai, China). 3-Aminopropyltrimethoxysilane (APTES 98%) and polyvinylpyrrolidone (PVP) were purchased from Alfa Aesar (USA). Fumonisin B_1 aptamers [19] and their partial complementary strands were synthesised by Shanghai Sangon Biological Science & Technology Company (Shanghai, China). Sample names and the DNA sequences are in Table 1.

2.2. Synthesis of magnetic nanoparticles

The carboxylation-functionalised magnetic nanoparticles applied here were prepared by a modified solvothermal reaction using the reduction of $FeCl_3$ with sodium acetate as an alkali source and biocompatible trisodium citrate as an electrostatic stabiliser [22]. The details of this preparation are shown in Supplementary section. Typically, $FeCl_3$ (0.65 g, 4.0 mmol) and trisodium citrate (0.40 g, 1.36 mmol) were first dissolved in ethylene glycol (20 mL); afterwards, NaAc (1.20 g) was added with stirring. The mixture was stirred vigorously for 30 min and then sealed in a Teflon-lined stainless-steel autoclave. The autoclave was heated to 198 °C and maintained for 12 h, then allowed to cool to room temperature. The black products were washed with ethanol and de-ionised water three times. The carboxylation-functionalised magnetic nanoparticles were characterised by TEM.

2.3. Preparation of AuNPs and AuNPs–MB

The 15 nm AuNPs were synthesised by a common method, using the sodium citrate reduction of developed gold ions [23]. The details of this preparation are shown in Supplementary section. The procedure for binding AuNPs with MB oligonucleotides was adapted from the previously reported protocol [24,25]. This protocol was based on the Au–S interaction between the gold lattice and thiolated oligonucleotides. Briefly, the 100 nM MB was added to AuNPs solution with 10 mM PBS (pH 7.4). After standing for 16 h, the AuNPs–MB complexes were "aged" with salts (0.1 M NaCl, 10 mM phosphate, pH 7.0) for 40 h. The solution was then centrifuged at 15,000 rpm for 30 min. The supernatant was removed, and the reddish solid at the bottom of the tube was dispersed in the binding buffer (10 mM Tris · HCl, pH 8.0, 100 mM KCl and 1 mM $MgCl_2$) for subsequent experiments.

2.4. Synthesis and surface modification of $NaYF_4$:Yb, Ho UCNPs

$NaY_{0.78}F_4$:$Yb_{0.20}$, $Ho_{0.02}$ UCNPs were synthesised according to the method described by our previous work with some modifications [26]. The details of this preparation are shown in Supplementary section. Then, surface modification of $NaY_{0.78}F_4$:$Yb_{0.20}$, $Ho_{0.02}$ UCNPs were performed with PVP-assisted cap silica on the surface of the UCNPs [27,28]. In a 250 mL flask, 60 mg of UCNPs and 60 mg PVP were dispersed in 60 mL of 3-propanol by sonication and agitation for 40 min, then 2.5 mL of ammonia and 20 mL of water were added to the flask. The mixture was then maintained at 35 °C under vigorous stirring. A solution containing 20 mL of 3-propanol and 75 μL of TEOS was added dropwise to the mixture over a period of 1 h, and the reaction was continued for another 2 h. To synthesise the amino-modified UCNPs, a solution containing 30 mL of 3-propanol and 200 μL of APTES was added dropwise into the suspension, and the reaction was

Table 1
The sequences of molecular beacon, FB_1-aptamers and complementary oligonucleotides.

Sample name	Sequence
MB	5′-SH-$(CH_2)_6$-GCTCG CCA GCT TAT TCA ATT CGAGC-$(CH_2)_6$-H_2N-3′
FB_1-aptamers	5′-Biotin-$(CH_2)_6$-ATA CCA GCT TAT TCA ATT AAT CGC ATT ACC TTA TAC CAG CTT ATT CAA TTA CGT CTG CAC ATA CCA GCT TAT TCA ATT AGA TAG TAA GTG CAA TCT-3′
Complementary oligonucleotides	5′-AAT TGA ATA AGC TGG-3′

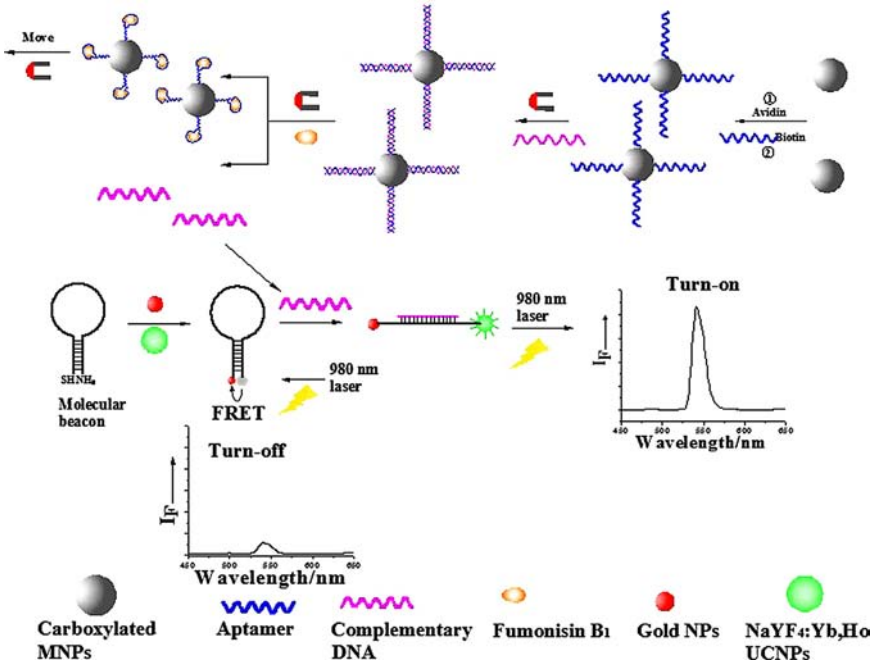

Fig. 1. Schematic illustration of the fluorescence resonance energy transfer between $NaYF_4$: Yb, Ho UCNPs and AuNPs based on molecular beacons for fumonisin B_1 sensing.

continued for 1 h. When the reaction was terminated, the product was "aged" for 2 h at room temperature. The precipitates were then separated by centrifugation, washed with ethanol three times, and dried at 60 °C for 12 h to obtain amino-functionalised UCNPs. Thus, the amino-modified $NaY_{0.78}F_4$:$Yb_{0.20}$, $Ho_{0.02}$ UCNPs were formed.

2.5. Synthesis of AuNPs–MB–UCNPs

The amino-modified UCNPs conjugated with an amino-group at the 3′ end of the molecular beacon were fabricated by the classic glutaraldehyde method [29]. Typically, 10 mg of UCNPs were dispersed in 5 mL of 10 mM phosphate buffer solution (pH 7.4) by ultrasonication for 20 min. A solution of 25% glutaraldehyde (1.25 mL) was then added to the mixture. The mixture was shaken slowly at room temperature for 1 h, and the UCNPs were centrifuged and washed with PBS three times to remove the physically adsorbed glutaraldehyde. Subsequently, the freshly synthesised and purified AuNPs–MB conjugates (1 mL) were added to the modified UCNPs; the mixture was shaken slowly on a shaking table at room temperature for 12 h, and then washed with the buffer three times. Finally, the mixture was resuspended in buffer (10 mM Tris · HCl, pH 8.0, 100 mM KCl and 1 mM $MgCl_2$) by centrifugation at 6000 rpm for 15 min for use in subsequent experiments.

2.6. Assay procedure of the proposed method

Carboxylation-functionalised MNPs were conjugated with FB_1-aptamers in two steps. First, avidin-conjugated MNPs were prepared: 100 μL of 0.1 mg mL^{-1} avidin solution in 10 mM phosphate buffer solution (PBS) of pH 7.4 was mixed with 100 μL of 2 mg mL^{-1} carboxylation-functionalised MNPs solution in the same buffer. The mixture was activated with 50 μL of 0.2 mg mL^{-1} EDC and 25 μL of 0.2 mg mL^{-1} NHS for 10 min at room temperature, and the reaction was continued for 2 h at 37 °C in a reciprocating oscillator. The avidin-conjugated MNPs were purified by magnetic force and washed with PBS three times, and the supernatant was discarded each time. Subsequently, 100 nM biotinylated FB_1-aptamers were immobilised on the surface of avidin-conjugated MNPs for 12 h at 37 °C through a biotin–avidin affinity reaction, and the unreacted biotinylated FB_1-aptamers were separated and rinsed with PBS. Then, 200 μL solution of the above FB_1-aptamer and MNPs conjugates and 200 nM complementary oligonucleotides were hybridised for 30 min at 37 °C, and the unreacted complementary oligonucleotides were removed by an external magnet. In a typical measurement, different concentrations of FB_1 were added to the 200 μL solution of the duplex of FB_1-aptamer and complementary oligonucleotides with the MNPs in 10 mM PBS and incubated for 30–40 min. Then, the supernatant of the complementary oligonucleotides was liberated from the MNPs with an external magnet and transferred into the 200 μL solution of AuNPs–MB–UCNPs. The fluorescence intensity of the AuNPs–MB–UCNPs solution was measured after hybridisation of the complementary oligonucleotides and the loop of the MB for approximately 1 h.

2.7. Sample preparation and measurement

A total of 15 naturally contaminated maize samples obtained from local agricultural markets were treated using an enzyme-linked immunosorbent assay method. Briefly, each sample was ground with a high-speed disintegrator and passed through a test sieve (1 mm aperture). Five grams of each ground sample and 5 g of NaCl were introduced into a 100 mL flask, and the extracting solution (7:3 methanol:H_2O; v-v) was filled to the mark and completely mixed with the compound. The mixture was then transferred into the cup of a homogeniser. The mixture was then stirred at high-speed and extracted for 2 min. Next, the resulting solution was filtered, and 10.0 mL of filtrate was transferred into a 50 mL flask. Water was filled to the mark, and the flask contents were mixed to homogeneity. The resulting mixture was further filtered through glass fibre filter paper until the filtrate was clear. The filtrate was collected in a clean container to measure the FB_1 content using the above mentioned procedure and validated by commercially available ELISA. For the standard addition and recovery experiment, the standard FB_1 was introduced into the maize ground samples before adding the extracting solution.

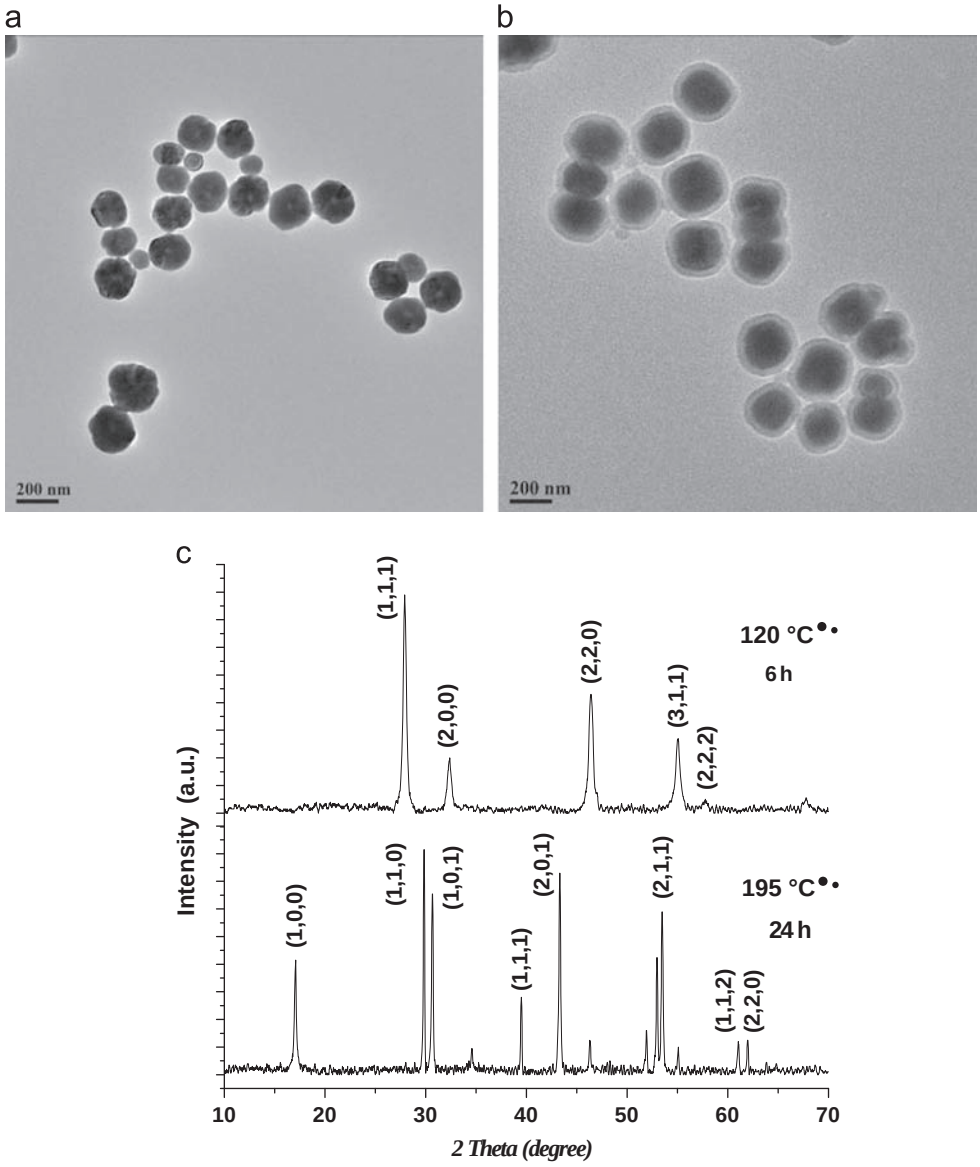

Fig. 2. TEM images of NaYF4: Yb, Ho UCNPs (a) and NaYF4: Yb, Ho UCNPs @ SiO_2 (b); XRD patterns of cubic α-phase NaYF4:Yb, Ho UCNPs synthesised at 120 °C for 6 h and hexagonal β-phase NaYF4:Yb, Ho UCNPs synthesised at 195 °C for 24 h (c).

3. Results and discussion

3.1. Principle of the UCNPs-based FRET aptasensor for fumonisin B_1

We developed a sensitive and novel FRET system for detection of FB_1 with $NaYF_4$: Yb, Ho UCNPs and AuNPs as the FRET pair. As shown in Fig. 1, the FB_1 aptamers were first linked to the magnetic nanoparticles; the complementary oligonucleotides were then hybridised with the aptamers. In the presence of the FB_1, the aptamers could be separated from their complementary oligonucleotides as they bound to the FB_1, which competitively replaced and released the complementary oligonucleotides. The FB_1-specific aptamers were selected by SELEX (systematic evolution of ligands by exponential enrichment) [19]. To further study the sensing process of FB_1 and FB_1-specific aptamers, circular dichroism (CD) was used to confirm the conformational variations of the aptamers, and the details were shown in Supplementary section (Fig. S1). Each released complementary oligonucleotide could then be hybridised to the loop of the MB. The quencher (AuNPs) was attached to the 5′ end of the MB, which can quench the fluorescence of the donor (UCNPs) attaching to the 3′ end of the MB through the resonance energy transfer in the absence of the complementary oligonucleotides. In the presence of the complementary oligonucleotides, the hybridisation between the loop and the target was longer and more stable than the stem. Thus, the MB underwent spontaneous conformational change and caused the UCNPs and AuNPs to detach from each other, restoring the upconversion fluorescence.

3.2. Characterisation of the prepared upconversion nanoparticles and magnetic nanoparticles

A typical TEM image of the bare UCNPs synthesised before silica coating is shown in Fig. 2a; the UCNPs are well-dispersed and uniform in size with an average diameter of approximately 150 nm. It should be noted that the UCNPs synthesised under relatively stringent conditions (for example, at 195 °C for 24 h) present a regular spherical shape that is beneficial to their further application in biomolecules. After surface modification by SiO_2, the size of the UCNPs was increased to approximately 200 nm due to the formation of a thin silica layer on the surface of the bare UCNPs in Fig. 2b.

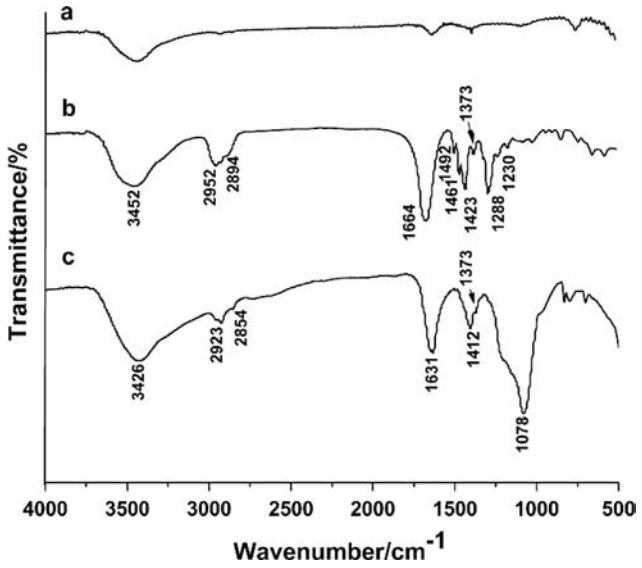

Fig. 3. FT-IR spectra of the as-prepared $NaYF_4$ Yb, Ho upconversion nanoparticles (a), PVP (b) and SiO_2/PVP/$NaYF_4$: Yb, Ho upconversion nanoparticles (c).

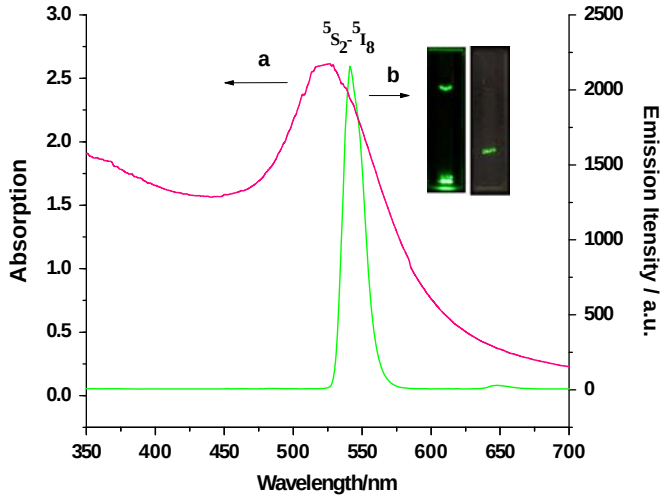

Fig. 4. UV–vis absorption spectrum of AuNPs (a) and upconversion fluorescence emission spectrum of $NaYF_4$: Yb, Ho UCNPs @SiO_2 (b); photograph of naked-eye visible green upconversion fluorescence of $NaYF_4$:Yb, Ho UCNPs @SiO_2 in a transparent aqueous colloid solution.

During the experiment, we found that the reaction time and temperature were two primary influencing factors in the phase transition of $NaYF_4$ UCNPs. The XRD patterns of $NaYF_4$: Yb, Ho UCNPs synthesised at various reaction times and temperatures are presented in Fig. 2c. When the reaction time was maintained at 120 °C for 6 h, the XRD pattern matched well with that of the cubic α-phase of $NaYF_4$ (JCPDS no. 77-2042). When the reaction temperature was increased to 195 °C and the time increased to 12 h, new diffraction peaks that can be assigned to the hexagonal β-phase of $NaYbF_4$ (JCPDS no. 16-0334) are observed; the above phenomena may be attributed to the cubic-to-hexagonal phase transition. When the reaction time was increased, the peaks belonging to the hexagonal β-phase all significantly enhanced, whereas those corresponding to the cubic α-phase were weakened. However, the UCNPs cannot be transformed from the cubic α-phase to the hexagonal β-phase completely over 24 h at 195 °C.

Polyvinylpyrrolidone (PVP) was used in this work as both the chelating agent and stabiliser to synthesise $NaYF_4$ nanoparticles with controlled size and shape in addition to suitable surface properties and aqueous solubility [28]. In the FT-IR spectrum of the PVP stabilised nanoparticles (Fig. 3), the broad absorption band located at 3426 cm^{-1} could be assigned to –OH groups from the absorbed water. The characteristic IR peaks located at 1631 cm^{-1} could be assigned to the C=O stretching, indicating the presence of PVP on the surface of the nanoparticles. The IR peaks at 2923∼2854 cm^{-1} and 1412 cm^{-1} correspond to the stretching and bending of the $-CH_2$ groups, and the peak at 1078 cm^{-1} corresponds to the Si-O-Si stretching, confirming the existence of silica on the nanoparticles. It has been reported that the IR absorption peaks of PVP show a small red-shift when the C=O groups are bound to metal ions [30,31]. The IR absorption peaks assigned to the C=O groups of PVP/$NaYF_4$ nanocrystals were red-shifted compared to that of pure PVP, indicating that the PVP was adsorbed onto the nanocrystals as a ligand coordinating with the lanthanide ions.

The carboxylation-functionalised magnetic nanoparticles used here were obtained with Na_3Cit. TEM (Fig. S2a), FT-IR (Fig. S2b) and XRD (Fig. S2c) were used to characterise the as-synthesised magnetic nanoparticles.

3.3. Binding studies of AuNPs–MB–UCNPs

It is well-known that AuNPs show good absorption properties in the visible region. The AuNPs suspension used in this work displays a strong absorption band at approximately 530 nm (Fig. 4a); thus, it is a suitable energy acceptor/quencher in the FRET-based assays. Fig. 4b shows the UC fluorescence spectrum of the $NaYF_4$:Yb, Ho UCNPs @SiO_2 suspension. The green emission at 542 nm in the emission band is found in the fluorescence spectrum; thus, the UCNPs with the strong green emission are very suitable for use as an energy donor in the FRET-based assays. The UV–vis absorption spectrum of the AuNPs clearly overlaps with the UC fluorescence emission spectrum of $NaYF_4$:Yb, Ho UCNPs @SiO_2, thus making the FRET between the $NaYF_4$:Yb, Ho UCNPs @SiO_2 (donor) and the AuNPs (acceptor) possible.

AuNPs–MB–UCNPs were assembled by the Au–S covalent interaction between the gold lattice and the 5′-thiolated molecular beacon [32], and the amino-modified UCNPs conjugated with the 3′-amination molecular beacon. To verify the successful coupling, the AuNPs–MB–UCNPs complex was characterised by TEM imaging. As shown in Fig. 5a, the 15 nm AuNPs were well-dispersed and many AuNPs were present on the surface of the UCNPs in Fig. 5b; this indicated that the gold nanoparticles were drawn to the UCNP surface through binding with the molecular beacon. In contrast, in the absence of molecular beacon, most AuNPs were far from the UCNPs, and only a few AuNPs were conjugated with the UCNPs by non-specific absorption (Fig. 5c).

3.4. Optimisation of quencher concentration

To identify the optimal quenching concentration of the molecular beacon, a comparative study was performed using a constant concentration of the sample and various concentrations of AuNPs. The detection was based on fluorescence restoration following the addition of various volumes of AuNPs that bind to the molecular beacon as the quencher. As shown in Fig. 6, the restoration of the fluorescence of the molecular beacon using $NaYF_4$,Yb/Ho UCNPs as the donor was related to the concentration of the AuNPs solution; the fluorescence intensity reached a maximum upon the addition of eight times the dilution of AuNPs solution and decreased at higher concentrations of the AuNPs solution. With a small quantity of AuNPs binding to the molecular beacon, the fluorescence restoration was limited as a result of the low quenching efficiency. When the concentrations of the donor and quencher were optimised, the fluorescence restoration reached a maximum. However, if the

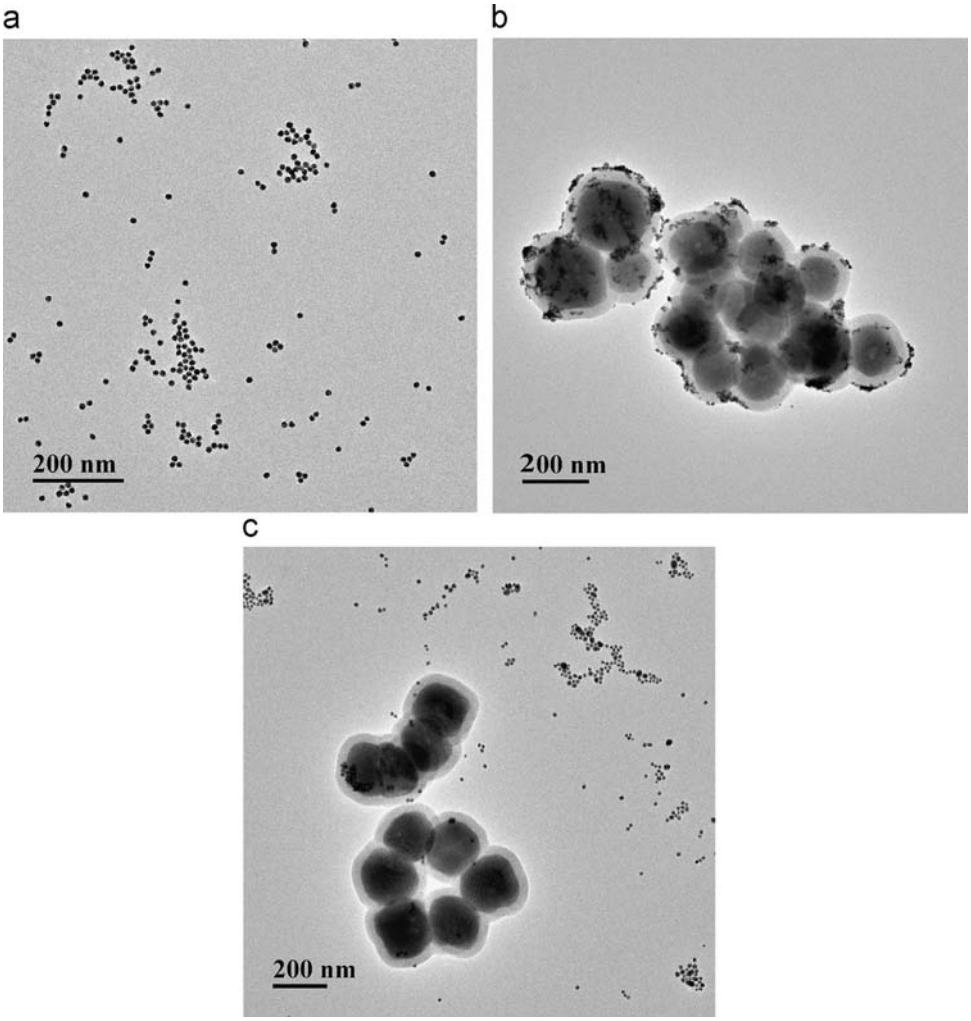

Fig. 5. TEM image of AuNPs (a) and TEM image of AuNPs–UCNPs with MB (b), TEM image of AuNPs–UCNPs without MB (c).

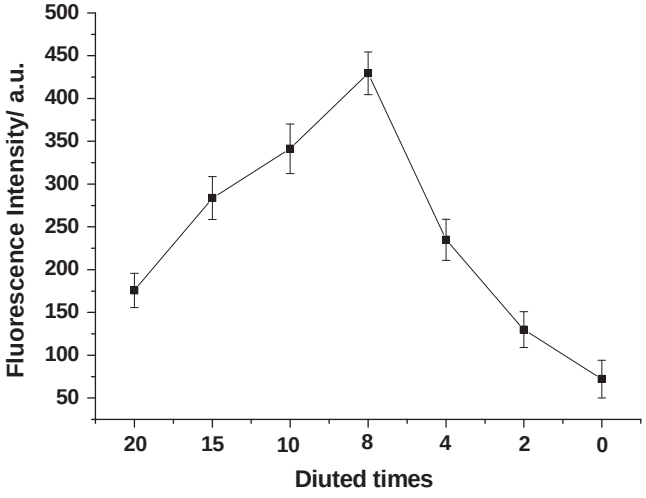

Fig. 6. Fluorescence resonance energy transfer with different concentration of AuNPs binding to the molecular beacon.

quantity of AuNPs was increased, the fluorescence intensity decreased because the coloured AuNPs solution overwhelmed the fluorescence. Another reason is that the quencher concentration far exceeded the donor concentration, and the fluorescence restoration was impeded.

3.5. Recognition of MB-complementary DNA

To confirm that the fluorescence restoration was caused by complementary oligonucleotides, several control experiments were performed. As shown in Fig. 7a, the upconversion fluorescence intensity showed only a slight change when the AuNPs and UCNPs coexisted in the absence of MB. The upconversion fluorescence quenching efficiency was also slight when the MB was hybridised with complementary oligonucleotides before the addition of the AuNPs and UCNPs (Fig. 7b). Some experiments indicated that the fluorescence recovery of the AuNPs and UCNPs complex solution in the presence of the complementary oligonucleotides resulted from a change in the MB conformation, the distance between the donor and acceptor was increased (Fig. 7c). However, the upconversion fluorescence was significantly quenched by the AuNPs because the AuNPs and UCNPs complex bound tightly with the MB (Fig. 7d).

3.6. Analytical procedure and performance

The fluorescence intensity of upconversion fluorescence increased with increasing concentrations of the complementary oligonucleotides. It is reasonable to assume that the aptamers that are hybridised with the complementary oligonucleotides will combine with fumonisin B_1 to form a complex because of the high affinity between the aptamers and fumonisin B_1, thus causing the dissociation of some complementary oligonucleotides. The

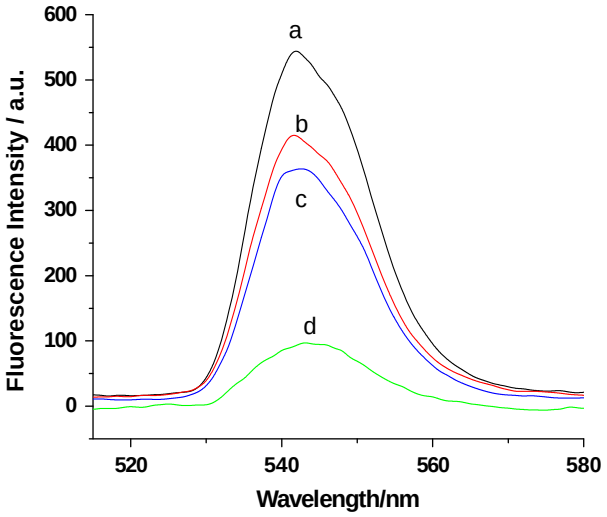

Fig. 7. Fluorescence spectra of AuNPs–UCNPs in the absence of MB (a); MB hybridised with complementary oligonucleotides, then the AuNPs and UCNPs were added (b); both AuNPs and UCNPs binding to MB, then the complementary oligonucleotides were added (c); both AuNPs and UCNPs binding to MB together in the absence of the complementary oligonucleotides (d). Molecular beacon concentration: 50 nM. Excitation wavelength: 980 nm.

restoration of the UCNPs fluorescence was positively correlated with the concentration of fumonisin B_1. These data implied that the hybridisation of MB and the complementary oligonucleotides forced the MB to open and released the fluorescence of UCNPs in a concentration-dependent manner.

For the detection of FB_1, the fluorescence intensity was weakest in the absence of FB_1, and the fluorescence signals of the molecular beacon were gradually restored with increasing concentrations of FB_1. Under optimal conditions, the concentration of mycotoxin is proportional to the increased fluorescence intensity (ΔI), where ΔI represents the difference of the upconversion fluorescence intensity excited by a 980 nm laser in the absence and in the presence of FB_1. As shown in Fig. 8, when the concentrations of FB_1 are in the range of 0.01–100 ng mL^{-1}, the relationship is linear with respect to the upconversion fluorescence intensity ($\Delta I = 187.59$ ln C+403.84; $R = 0.9981$). Statistical analysis revealed that the detection limit of FB_1 is equal to 0.01 ng mL^{-1}, as estimated using 3σ. This value is desirable for the detection of FB_1 in various types of foods with respect to the maximum acceptable standards of the FAO/WHO/FDA (2 mg kg^{-1}). The result is also better than those of most existing detection methods. The details of comparison with other bioassay methods were shown in Supplementary section (Table S1). The relative standard deviation of FB_1 detection is equal to 4.24% (1 ng mL^{-1}, $n = 11$), indicating that the developed method exhibited good reproducibility.

3.7. Analytical application

The feasibility of applying the aptasensors based on fluorescence resonance energy transfer techniques to measure the FB_1 levels in naturally contaminated samples was studied using 15 specimens of maize obtained from local agricultural markets. These specimens were measured by the developed method and a commercially available ELISA method. The results were summarised in Fig. S3. The results showed that there was no significant difference between the two methods and that they were highly correlated. The sample pretreatment has been done to extract FB_1 from the food matrices, most of the interfering substances such as protein and fat were removed from the extracting solution. Although, maybe there were some salt ions, such as Na^+, K^+, Ca^{2+}, Mg^{2+}, Pb^{2+}, as well as even trace amounts of other small organic molecules, including vitamins and organic acids, still existing in the sample matrices. To evaluate the possibility of interference, the recoveries of FB_1 by a known quantity of standard addition were measured and the results were good and varied from 91.1% to 120% (see Table 2). Thus, it was indicated that FB_1 determination would be slightly effected by the interfering substances in food matrices after pretreatment.

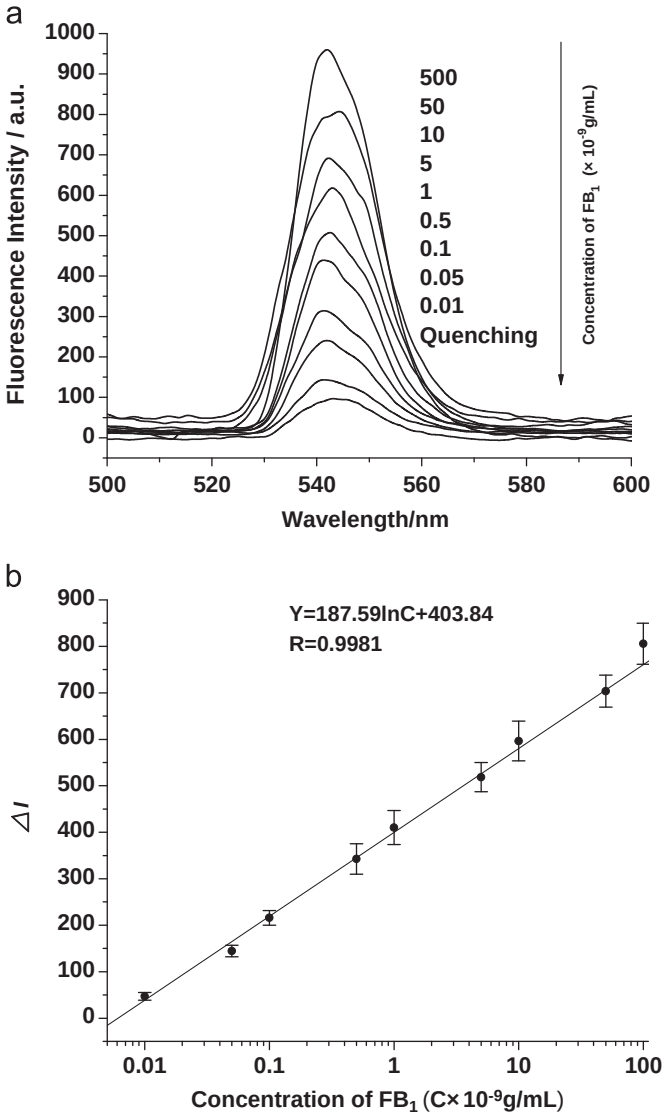

Fig. 8. Typical recording output for the detection of different concentrations of FB_1 by the developed method (a). Standard curve of the fluorescence intensity (ΔI) versus the FB_1 concentration was measured by the developed method (b).

Table 2
Recovery results for the added standard FB_1 from maize samples obtained by the developed method.

Sample	Background content (ng mL^{-1})	Added concentration (ng mL^{-1})	Detected concentration (ng mL^{-1})	Recovery ratio %
No. 1	0.357	0.05	0.413	112
		5	4.912	91.1
		50	51.125	101.5
No. 2	7.482	0.05	7.422	120
		5	13.035	111
		50	55.128	95.29
No. 3	74.241	0.05	74.287	92
		5	78.931	93.8
		50	123.345	98.21

4. Conclusions

In conclusion, we demonstrated that AuNPs can act as an highly efficient quencher for functionalised $NaYF_4$: Yb, Ho UCNPs and based on this phenomenon, an extraordinarily sensitive and specific FRET-based biosensing platform has been successfully developed. Several reasons could explain the excellent analytical performance of the proposed sensing platform. First, the ultra-high fluorescence quenching efficiency of the AuNPs on UCNPs led to low background and resulted in high sensitivity. Second, $NaYF_4$: Yb, Ho UCNPs were firstly to be used as donor in the FRET system until now, they did not induce autofluorescence and light scattering, and as a result, the signal-to-noise ratio was greatly improved. In addition, the single strong green upconversion fluorescence emission guarantees sensitive fluorescence "turn-on" upon the addition of target molecules at rather low concentrations. Importantly, the proposed method was highly sensitive to FB_1 detection with high specificity and stability of aptamer.

Acknowledgement

This work was partly supported by the S&T Supporting Project of Jiangsu Province (BE2011621), and Guangdong Province (2011B031500025), National Science and Technology Support Program of China (2012BAK08B01), and Research Fund for the Doctoral Program of Higher Education (20110093110002), NCET-11-0663, and JUSRP51309A.

Appendix A. Supplementary material

Supplementary data associated with this article can be found in the online version at http://dx.doi.org/10.1016/j.talanta.2013.07.016.

References

[1] S. Tyagi, S.A. Marras, F.R. Kramer, Nat. Biotechnol. 18 (2000) 1191–1196.
[2] K.M. Wang, Z.W. Tang, C.Y.J. Yang, Y.M. Kim, X.H. Fang, W. Li, Y.R. Wu, C. D. Medley, Z.H. Cao, J. Li, P. Colon, H. Lin, W.H. Tan, Angew. Chem. Int. Ed. 48 (2009) 856–870.
[3] L. Tan, Y. Li, T.J. Drake, L. Moroz, K.M Wang, J. Li, A. Munteanu, C.Y.J. Yang, K. Martinez, W.H. Tan, Analyst 130 (2005) 1002–1005.
[4] G. Bonnet, S. Tyagi, A. Libchaber, F.R. Kramer, Proc. Natl. Acad. Sci. USA 96 (1999) 6171–6176.
[5] S. Wang, B.S. Gaylord, G.C. Bazan, J. Am. Chem. Soc. 126 (2004) 5446–5451.
[6] G.S. Yi, G.M. Chow, Adv. Funct. Mater. 16 (2006) 2324–2329.
[7] O. Ehlert, R. Thomann, M. Darbandi, T. Nann, ACS Nano 2 (2008) 120–124.
[8] F. Wang, X.G. Liu, Chem. Soc. Rev. 38 (2009) 976–989.
[9] S.J. Wu, N. Duan, C.Q. Zhu, X.Y. Ma, M. Wang, Z.P. Wang, Biosens. Bioelectron. 30 (2011) 35–42.
[10] S.J. Wu, N. Duan, X.Y. Ma, Y. Xia, H.X. Wang, Z.P. Wang, Q. Zhang, Anal. Chem. 84 (2012) 6263–6270.
[11] L.Y. Wang, R.X. Yan, Z.Y. Hao, L. Wang, J.H. Zeng, H. Bao, X. Wang, Q. Peng, Y. D. Li, Angew. Chem. Int. Ed. 44 (2005) 6054–6057.
[12] C.H. Liu, Z. Wang, H.X. Jia, Z.P. Li, Chem. Commun. 47 (2011) 4661–4663.
[13] H.Q. Chen, J.C. Ren, Talanta 99 (2012) 404–408.
[14] M.F. Dutton, Pharmacol. Ther. 70 (1996) 137–161.
[15] W.P. Norred, E. Wang, H. Yoo, R.T. Riley, A.H. Merrill, Mycopathologia 117 (1992) 73–78.
[16] W.S. Khayoon, B. Saad, B. Salleh, N.A. Ismail, N.H.A. Manaf, A.A. Latiff, Anal. Chim. Acta 679 (2010) 91–97.
[17] G.S. Shephard, J. Chromatogr. A 815 (1998) 31–39.
[18] S. Wang, Y. Quan, N.J. Lee, I.R. Kenndye, J. Agric. Food Chem. 54 (2006) 2491–2495.
[19] M. McKeague, C.R. Bradley, A. De Girolamo, A. Visconti, J.D. Miller, M. C. DeRosa, Int. J. Mol. Sci. 11 (2010) 4864–4881.
[20] C.M. Maragos, J. Agric. Food. Chem. 43 (1995) 390–394.
[21] M. Wang, W. Hou, C.C. Mi, W.X. Wang, Z.R. Xu, H.H. Teng, C.B. Mao, S.K. Xu, Anal. Chem. 81 (2009) 8783–8789.
[22] J. Liu, Z.K. Sun, Y.H. Deng, Y. Zou, C.Y. Li, X.H. Guo, L.Q. Xiong, Y. Gao, Y. Li, D. Y. Zhao, Angew. Chem. Int. Ed. 48 (2009) 5875–5879.
[23] X.H. Ji, X.N. Song, J. Li, Y.B. Bai, W.S. Yang, X.G. Peng, J. Am. Chem. Soc. 129 (2007) 13939–13948.
[24] R. Elghanian, J.J. Storhoff, R.C. Mucic, R.L. Letsinger, C.A. Mirkin, Science 277 (1997) 1078.
[25] C.A. Mirkin, R.L. Letsinger, R.C. Mucic, J.J. Storhoff, Nature 382 (1996) 607.
[26] S.J. Wu, N. Duan, Z.P. Wang, H.X. Wang, Analyst 136 (2011) 2306–2314.
[27] W. Stöber, A. Fink, J. Colloid Interface Sci. 26 (1968) 62–69.
[28] Z.Q. Li, Y. Zhang, Angew. Chem. Int. Ed. 45 (2006) 7732–7735.
[29] X. Hun, Z.J. Zhang, Biosens. Bioelectron. 22 (2007) 2743–2748.
[30] S. Manju, K. Sreenivasan, J. Pharm. Sci-US 100 (2011) 504–511.
[31] J. Cha, P. Cui, J.K. Lee, J. Mater. Chem. 20 (2010) 5533–5537.
[32] G.M. Qiao, L.H. Zhuo, Y. Gao, L.J. Yu, N. Li, B. Tang, Chem. Commun. 47 (2011) 7458–7460.